ISSN: 0975-8585

Research Journal of Pharmaceutical, Biological and Chemical Sciences

Targeting Inflammation with Designed Hydrazone Derivatives: An Investigation through Molecular Docking, Synthesis and *In-vitro* Studies.

Rashmi T, Swaroopa HM, Vinutha S*, Bharath C, Punya M, Satish V, and Varshini SA.

Department of Pharmaceutical Chemistry, Bharathi College of Pharmacy, Bharathinagara, Mandya, Karnataka – 571422, India.

ABSTRACT

Inflammation is a complex biological response associated with numerous chronic diseases and current anti-inflammatory therapies are often limited by side effects and reduced efficacy over prolonged use. Hydrazone derivatives have emerged as biologically versatile scaffolds with reported anti-inflammatory potential. In the present study, a series of hydrazone derivatives were rationally designed and evaluated through molecular docking, chemical synthesis, structural characterization and *in-vitro* biological assays. Molecular docking against the Pokeweed inflammatory Protein (PDB ID: 3O8Y) was performed using AutoDock Vina to predict ligand-protein interactions and identify compounds with favorable binding energies. The structure–activity relationships (SAR) suggested that compounds decorated with electron-withdrawing nitro and electron-donating methoxy substituents displayed higher binding affinities. Six derivatives (C1, C2, C6, C7, C9 and C10) were synthesized via condensation of substituted acetophenones with hydrazone derivatives in ethanol under reflux. The purity and chemical structures were confirmed using IR, ^{1}H NMR and mass spectrometry. *In-vitro* anti-inflammatory activity was evaluated using the albumin denaturation assay, with diclofenac sodium as the standard. Compound C7 showed maximum inhibition with an IC_{50} value of 47.65 µg/mL, closely comparable to diclofenac (41.80 µg/mL), indicating potent anti-inflammatory activity. The results highlight the significance of substituent effects on biological activity and suggest that hydrazone derivatives can serve as promising lead compounds for the development of new anti-inflammatory drugs.

Keywords: Hydrazone derivatives, Inflammation, Molecular docking, Albumin denaturation assay, Anti-inflammatory activity, Structure–activity relationship.

https://doi.org/10.33887/rjpbcs/2025.16.5.7

Corresponding author

ISSN: 0975-8585

INTRODUCTION

Inflammation is a complex physiological response of the body to harmful stimuli, including pathogens, damaged cells, or irritants [1]. While acute inflammation is protective and essential for healing, chronic inflammation is implicated in the pathogenesis of numerous diseases, such as rheumatoid arthritis, inflammatory bowel disease, cardiovascular disorders, and cancer [2]. The inflammatory process is regulated by various mediators, including cytokines, prostaglandins, and enzymes such as cyclooxygenase (COX), making them potential therapeutic targets [3, 4]. Although nonsteroidal anti-inflammatory drugs (NSAIDs) and corticosteroids are widely used, their long-term use is often associated with significant adverse effects such as gastrointestinal irritation, renal dysfunction, and immunosuppression [5]. This highlights the need for novel anti-inflammatory agents with improved efficacy and safety profiles.

Hydrazone derivatives have emerged as a promising class of heterocyclic compounds exhibiting a broad spectrum of biological activities, including antimicrobial, antitumor, anticonvulsant, antitubercular, and anti-inflammatory effects [6]. Their structural flexibility, ability to form hydrogen bonds, and electronic characteristics make them suitable for binding with a wide range of biological targets [7]. Several studies have reported the potential of hydrazones as inhibitors of key pro-inflammatory enzymes, particularly COX-2 and inducible nitric oxide synthase (iNOS), thereby supporting their role as anti-inflammatory agents [8].

In this study, we report the rational design and synthesis of novel hydrazone derivatives aimed at targeting inflammation. A molecular docking approach was employed to predict the interaction of the designed compounds with inflammation-related targets, followed by synthesis and structural characterization using standard spectroscopic techniques. The synthesized compounds were then evaluated for their in vitro anti-inflammatory activity to identify potential lead candidates for further development.

MATERIALS AND METHODOLOGY

Molecular docking

Dataset ligands and ligand optimization

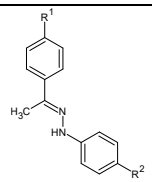

A designed Hydrazone derivative

Structure Code	R^1	R^2
C1	2,4-NO_2	H
C2	2,4-NO_2	m-OH
C3	2,4-NO_2	p-OH
C4	2,4-NO_2	o-OH
C5	2,4-NO_2	4-OCH_3
C6	2,4-NO_2	2-OCH_3
C7	2,4-NO_2	4-OCH_3, 3- NO_2
C8	P-Cl	H
C9	P-Cl	o-OH
C10	P-Cl	4-OCH_3, 3- NO_2

Table 1: Designed Hydrazone derivatives

The two-dimensional (2D) structures of ten selected compounds were designed using ACD/ChemSketch software [9]. These ligands were subsequently cleaned and subjected to three-dimensional (3D) geometry optimization before being saved in MDL Molfile format. The optimized ligands were then converted to the PDBQT format using the Open Babel chemistry toolbox to facilitate docking studies [10]. The 3D structure of Pokeweed Anti-inflammatory Protein (PAP) with PDB ID: 3O8Y was retrieved from the RCSB Protein Data Bank (https://www.rcsb.org) and prepared by removing unbound water molecules located more than 1 Å away, adding polar hydrogen atoms to satisfy valencies, and

modeling missing amino acid residues to stabilize side chains. Energy minimization of the complete protein structure was performed using the AutoDock suite within MGL Tools [11-13].

Molecular docking was carried out using AutoDock Vina. A docking grid was generated encompassing the active site based on the coordinates of the co-crystallized ligand (x = 34.76, y = 30.14, z = 10.58), as determined using MGL Tools and Pharmit (http://pharmit.csb.pitt.edu/) [14]. Docking simulations were conducted in the absence of water molecules for all ten ligand molecules. Post-docking, the ligand–protein interactions were analyzed using Discovery Studio Visualizer to assess binding at the active site. Binding affinities were evaluated based on docking scores, which reflect a composite of hydrophobic and hydrophilic interactions, van der Waals forces, metal-binding contributions, restricted rotatable bonds, and polar interactions with the receptor [15].

Synthesis Procedure

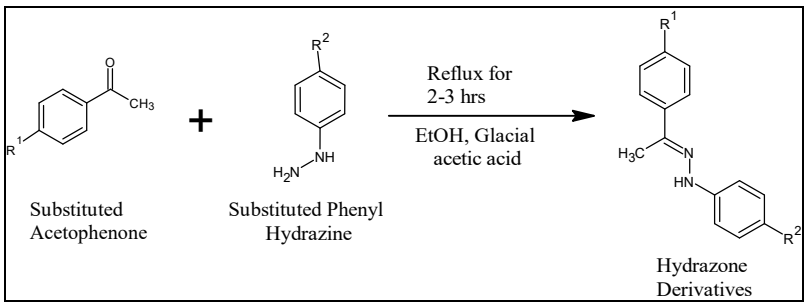

Scheme-I

Reaction Setup: In a 100 mL round-bottom flask, equip a magnetic stir bar and add equimolar amounts (1 mmol each) of Substituted acetophenone and the substituted phenylhydrazine.

Solvent and Catalyst Addition: Add 10-20 mL of absolute ethanol to the flask to dissolve the reactants. Then add 2–3 drops of glacial acetic acid to catalyze the condensation reaction.

Reflux: Heat the reaction mixture under reflux at 70–80 °C for 2-3hours with continuous stirring. Monitor the progress of the reaction by thin-layer chromatography (TLC), using a suitable solvent system (e.g., hexane:ethyl acetate, 7:3).

Completion and Cooling: After completion (as indicated by TLC), allow the reaction mixture to cool to room temperature. Add 15-20ml of icecold water then a precipitate of the hydrazone product typically forms.

Isolation: Filter the solid product under vacuum, and wash it with cold ethanol to remove any unreacted starting materials or impurities and recrystallise using ethanol.

Drying and Purification: Dry the crude product in a vacuum desiccator or oven at 40–50 °C. If required, recrystallize the product using ethanol or an appropriate solvent system to obtain the pure hydrazone derivative [16, 17].

Characterization

The melting points of the synthesized compounds were determined using the open capillary tube method with an electrically heated melting point apparatus. The values are reported in degrees Celsius (°C) and are uncorrected. The progress of the reaction and the purity of the compounds were monitored by thin-layer chromatography (TLC) using suitable solvent systems.

Structural elucidation of the synthesized compounds was carried out using various spectroscopic techniques. Infrared (IR) spectra were recorded on a Thermo Nicolet Nexus 670 Fourier Transform Infrared (FTIR) spectrometer over the range of 400-4000 cm^{-1} using potassium bromide (KBr) pellets, and the absorption frequencies are reported in cm^{-1}. Proton nuclear magnetic resonance (^1H NMR) spectra were obtained using a Bruker TopSpin NMR spectrometer with DMSO-d_6 as the solvent. Chemical shifts (δ) are

expressed in parts per million (ppm) relative to tetramethylsilane (TMS) as the internal standard. Mass spectra were recorded on a Shimadzu LC-MS 8030 mass spectrometer, and the fragmentation patterns were interpreted to confirm the molecular weights and structures of the synthesized compounds.

***In-vitro* Anti-inflammatory activity**

Albumin Denaturation Assay

The *in-vitro* anti-inflammatory activity of the synthesized compound was evaluated using the albumin denaturation assay. This method is based on the principle that denaturation of proteins such as albumin, contributes to inflammation and compounds that inhibit this process may possess anti-inflammatory potential. In this assay, bovine serum albumin (BSA) was used as the model protein [18].

A 1% aqueous solution of BSA was prepared and mixed with phosphate buffer saline (PBS, pH 6.4) and 10µg/ml concentrations of the test compound, previously dissolved in DMSO and diluted with distilled water. The reaction mixture consisted of 0.5 mL of 1% BSA, 0.5 mL of phosphate buffer, and 1 mL of the test solution. A control sample was prepared using distilled water in place of the test compound, while a standard solution containing diclofenac sodium at similar concentrations was used for comparison.

All reaction mixtures were incubated at 37 °C for 20 minutes, followed by heating at 70 °C for 5 minutes in a water bath to induce protein denaturation. After heat treatment, the samples were cooled to room temperature, and the turbidity (due to protein denaturation) was measured spectrophotometrically at 660 nm using a UV-visible spectrophotometer.

The percentage inhibition of protein denaturation was calculated using the formula:

$$\% \, Inhibition = \frac{A \, control - A \, sample}{A \, control} \times 100$$

where $A_{control}$ is the absorbance of the control reaction (without test compound), and A_{sample} is the absorbance in the presence of the test compound. A higher percentage of inhibition indicates better anti-inflammatory activity. Each sample was tested in triplicate to ensure accuracy and reproducibility of results[19,20].

RESULT AND DISCUSSION

Molecular docking

Molecular docking studies were conducted to investigate the potential interactions between the target protein and the designed ligand dataset. The active site residues of the Pokeweed Antiviral Protein (PDB ID: 3O8Y) were predicted using the Computed Atlas of Surface Topography of Proteins (CASTp) server. Both the target protein and ligand molecules were geometrically optimized prior to docking.

S. Code	Binding energy	No. of H Bonds	Interacting Amino acids	Bond length
C1	**-7.2**	3H	LYS:319, MET:231, GLN:656	4.94, 3.53, 4.84
C2	**-7.0**	2H	ASP:285, LEU:244	4.12, 4.53
C3	**-6.7**	1H	LYS:631	6.59
C4	-6.7	1H	LYS:423	3.72
C5	-6.5	2H	TRP:605, SER:215	5.10, 4.40
C6	**-6.8**	2H	ARG:246, THR:444	6.33, 4.63
C7	**-6.8**	2H	ARG:246, ARG:438	5.16, 3.66
C8	-6.3	-	-	-
C9	-6.4	1H	ASP:54	4.29
C10	-6.6	1H	THR:444	4.34
native	**-7.4**	2H	ARG:246, ASP:285	4.40, 3.88

Table 2: Binding interactions of Hydrazone derivatives against (PDB ID: 3O8Y)

ISSN: 0975-8585

All ten compounds were docked into the predicted active site of the target protein using AutoDock Vina. The docking simulations not only facilitated the identification of key binding interactions but also provided insight into possible conformational adaptations of the ligands within the protein environment.

For each protein-ligand complex, approximately 100 different binding conformations were generated using the AutoDock suite within MGL Tools. Among these, the conformation exhibiting the lowest binding energy was selected as the best binding pose, indicating the most favorable interaction with the target protein.

Figure 1: 3D Structure of structure of Stable-5-Lipoxygenase (PDB ID: 3O8Y)

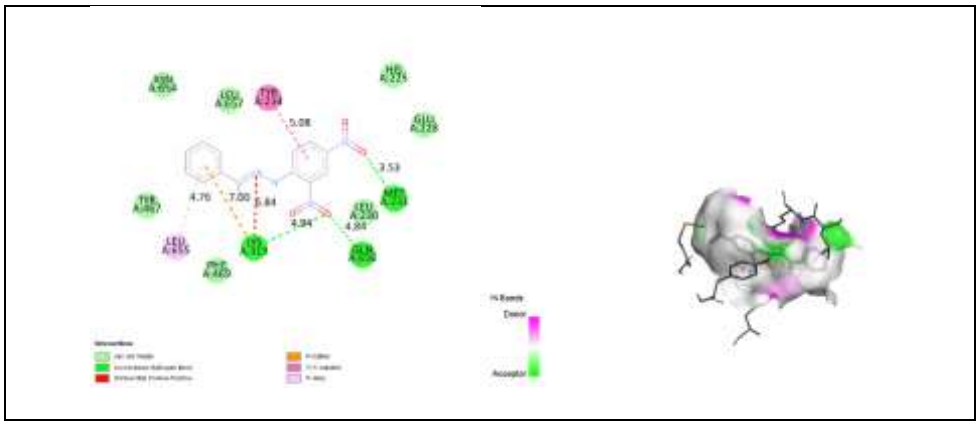

Figure 2: 2D and 3D Structure of the Compound C1 against PDB ID: 3O8Y

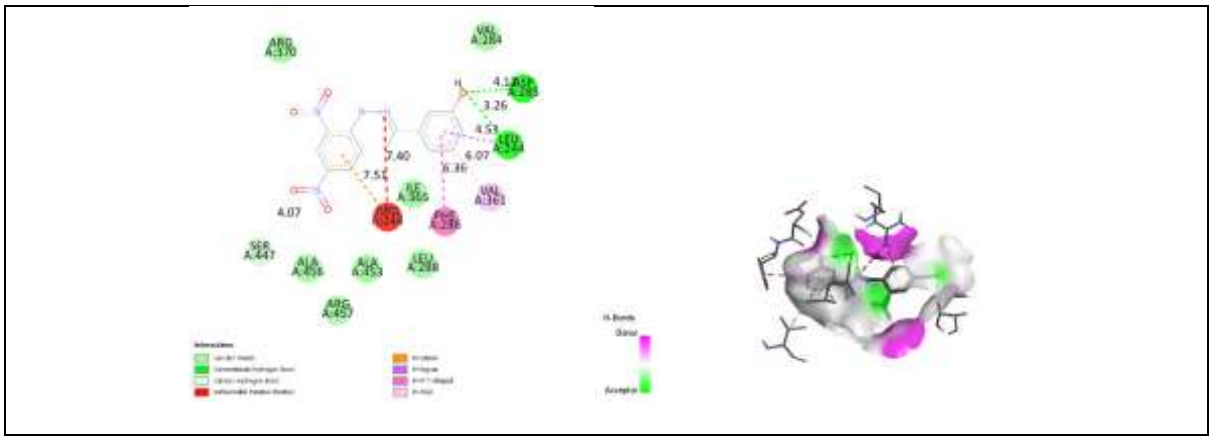

Figure 3: 2D and 3D Structure of the Compound C2 against PDB ID: 3O8Y

ISSN: 0975-8585

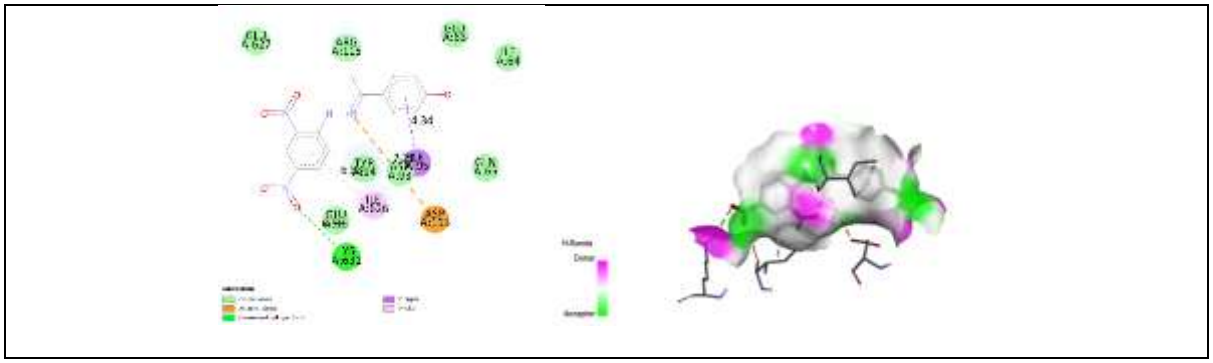

Figure 4: 2D and 3D Structure of the Compound C3 against PDB ID: 3O8Y

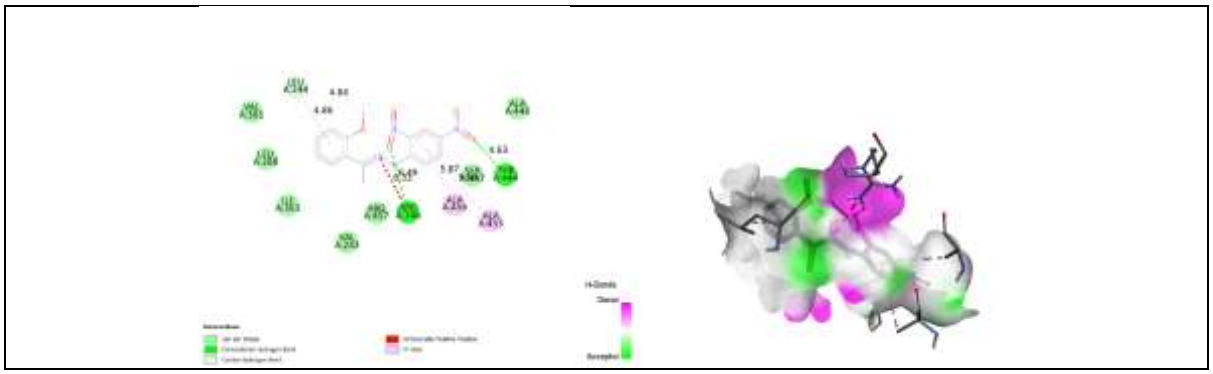

Figure 5: 2D and 3D Structure of the Compound C6 against PDB ID: 3O8Y

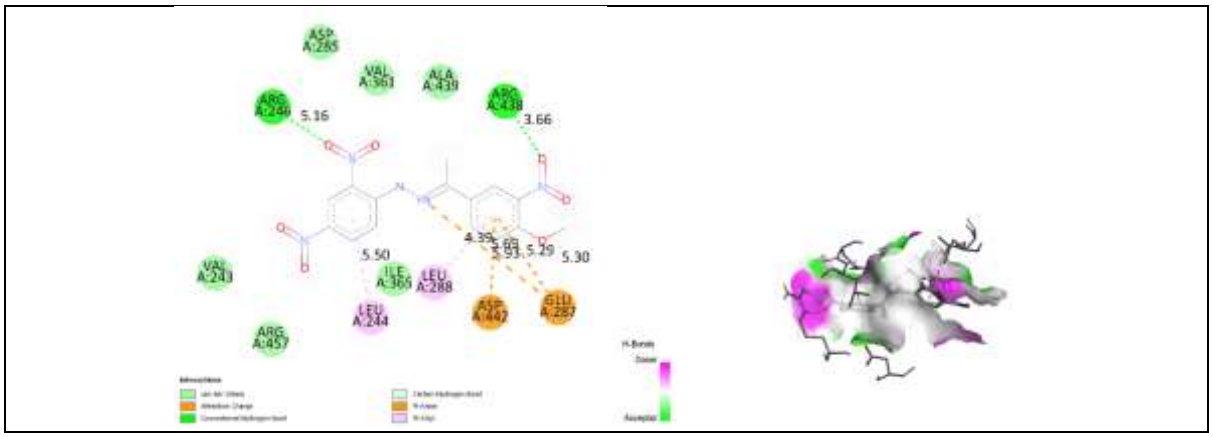

Figure 6: 2D and 3D Structure of the Compound C7 against PDB ID: 3O8Y

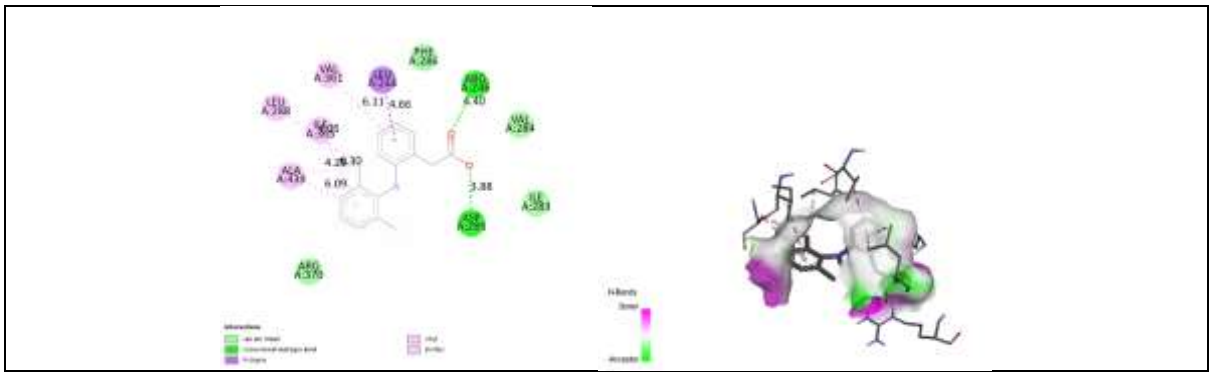

Figure 7: 2D and 3D Structure of the Diclofenac against PDB ID: 3O8Y

Synthesis

Code	R^1	R^2	Mol. Formula	Mol. wt ($g.mol^{-1}$)	Melting Point	% Yield
C1	H	2,4-NO_2	$C_{14}H_{12}N_4O_4$	300.274	110	72
C2	m-OH	2,4-NO_2	$C_{14}H_{12}N_4O_5$	316.273	210	78
C6	2-OCH_3	2,4-NO_2	$C_{15}H_{14}N_4O_5$	330.30	190	86
C7	4-OCH_3, 3- NO_2	2,4-NO_2	$C_{15}H_{13}N_5O_7$	375.297	200	79
C9	o-OH	P-Cl	$C_{14}H_{13}N2ClO$	260.721	160	83
C10	4-OCH_3, 3- NO_2	P-Cl	$C_{15}H_{14}N_3ClO_3$	319.745	180	75

Table 3: Physical Characterisation data of the Synthesized Compounds (C1, C2, C6, C7, C9 and C10)

Characterization

Compound C1: (2*E*)-1-(2,4-dinitrophenyl)-2-(1-phenylethylidene)hydrazine
IR (ν cm^{-1}): 3305 (N–H stretch, hydrazone), 3101 (C–H stretch, Aromatic), 1615 (C=N stretch, azomethine), 1523 and 1345 (N=O asymmetric and symmetric stretch for NO_2), 1490 (C=C stretch, aromatic), 1285 (C–N stretch), 765, 698 (Aromatic C–H bending).
^{1}H-NMR (DMSO-d_6, δ ppm): 11.45 (1H, s, NH, hydrazone), 8.52–8.25 (2H, m, Ar–H ortho to NO_2), 7.92–7.65 (3H, m, Ar–H), 7.45–7.26 (5H, m, phenyl ring protons), 2.38 (3H, s, –CH_3 attached to C=N).
Mass Spectrometry (ESI–MS): *m/z* 300.09 (M), *m/z* 301.10 (M+1, 100%).

Compound C2: 3-{(1*E*)-1-[2-(2,4-dinitrophenyl)hydrazinylidene]ethyl}phenol
IR (ν cm^{-1}): 3340 (O–H stretch, phenol), 3308 (N–H stretch, hydrazone), 3098 (C–H stretch, Aromatic), 1610 (C=N stretch, hydrazone), 1525 & 1340 (N=O asymmetric and symmetric stretches for NO_2), 1488 (C=C stretch, Aromatic), 1290 (C–N stretch), 755, 694 (Aromatic C–H bending).
^{1}H-NMR (DMSO-d_6, δ ppm): 11.20 (1H, s, phenolic –OH), 11.10 (1H, s, NH, hydrazone), 8.30–8.05 (2H, m, Ar–H ortho to NO_2), 7.82–7.55 (3H, m, Ar–H dinitro-phenyl), 7.45–7.10 (4H, m, aromatic protons of phenolic ring), 2.32 (3H, s, –CH_3 linked to azomethine carbon).
Mass Spectrometry (ESI–MS): *m/z* 316.07 (M), *m/z* 317.10 (M+1, 100%).

Compound C6: (2*E*)-1-(2,4-dinitrophenyl)-2-[1-(2-methoxyphenyl)ethylidene]hydrazine
IR (ν cm^{-1}): 3310 (N–H stretch, hydrazone), 3095 (C–H stretch, Aromatic), 2938 (C–H stretch,–OCH_3), 1608 (C=N stretch), 1518 & 1343 (N=O asymmetric and symmetric, NO_2 groups), 1495 (C=C stretch, Aromatic), 1265 (C–O stretch of –OCH_3), 1290 (C–N stretch), 758, 698 (Aromatic C–H bending).
^{1}H-NMR (DMSO-d_6, δ ppm): 11.35 (1H, s, NH of hydrazone), 8.24–8.05 (2H, m, Ar–H ortho to NO_2), 7.88–7.58 (3H, m, Ar–H of dinitrophenyl), 7.45–7.15 (4H, m, aromatic protons on anisole ring), 3.78 (3H, s, –OCH_3), 2.29 (3H, s, –CH_3 of azomethine carbon).
Mass Spectrometry (ESI–MS): *m/z* 330.10 (M), *m/z* 331.11 (M+1, 100%).

Compound C7: (2*E*)-1-(2,4-dinitrophenyl)-2-[1-(4-methoxy-3 nitrophenyl) ethylidene] hydrazine
IR (ν cm^{-1}): 3312 (N–H stretch, hydrazone), 3085 (C–H stretch, aromatic), 2945 (C–H stretch, –OCH_3), 1605 (C=N stretch, azomethine), 1520 & 1340 (N=O asymmetric and symmetric stretches, NO_2 groups), 1492 (C=C stretch, aromatic), 1263 (C–O stretch, methoxy), 1285 (C–N stretch), 760, 702 (aromatic C–H bending).
^{1}H-NMR (DMSO-d_6, δ ppm): 11.32 (1H, s, NH of hydrazone), 8.27–8.05 (3H, m, Ar–H on dinitrophenyl and nitrophenyl ring), 7.85–7.55 (3H, m, aromatic protons), 7.40–7.15 (2H, m, aromatic protons adjacent to –OCH_3), 3.82 (3H, s, –OCH_3), 2.30 (3H, s, –CH_3 of azomethine carbon).
Mass Spectrometry (ESI–MS): *m/z* 375.09 (M), *m/z* 376.10 (M+1, 100%).

Compound C9: 2-{(1*E*)-1-[2-(4-chlorophenyl)hydrazinylidene]ethyl}phenol
IR (ν cm^{-1}): 3365 (O–H stretch, phenol), 3298 (N–H stretch, hydrazone), 3090 (C–H stretch, aromatic), 2925 (C–H stretch, methyl), 1615 (C=N stretch, azomethine), 1495 (C=C stretch, Aromatic), 1270 (C–O stretch, phenolic), 760 (C–Cl stretch), 751, 696 (Aromatic C–H bending).
^{1}H-NMR (DMSO-d_6, δ ppm): 11.13 (1H, s, OH, phenolic), 10.62 (1H, s, NH, hydrazone), 7.80–7.48 (4H, m, Ar–H of 4-chlorophenyl), 7.25–6.95 (4H, m, Ar–H of phenolic ring), 2.34 (3H, s, –CH_3 attached to C=N).
Mass Spectrometry (ESI–MS): *m/z* 260.09 (M), *m/z* 261.10 (M+1, 100%), *m/z* 262.10 (M+2, ~35%).

Compound C10: (2*E*)-1-(4-chlorophenyl)-2-[1-(4-methoxy-3-nitrophenyl)ethylidene] hydrazine
IR (ν cm^{-1}): 3308 (N–H stretch, hydrazone), 3082 (C–H stretch, Aromatic), 2940 (C–H stretch, $–OCH_3$), 1603 (C=N stretch, azomethine), 1518 (N=O asymmetric stretch), 1343 (N=O symmetric stretch), 1490 (C=C stretch Aromatic), 1260 (C–O stretch of methoxy), 756, 698 (Aromatic C–H bending), 760 (C–Cl stretch).
^{1}H-NMR (DMSO-d_6, δ ppm): 11.25 (1H, s, NH, hydrazone), 8.20–7.95 (3H, m, Ar–H near nitro/methoxy groups), 7.78–7.50 (4H, m, Ar–H from chlorophenyl ring), 7.45–7.15 (2H, m, aromatic protons), 3.81 (3H, s, $–OCH_3$), 2.31 (3H, s, $–CH_3$ attached to C=N).
Mass Spectrometry (ESI–MS): *m/z* 319.10 (M), *m/z* 320.12 (M+1, 100%), *m/z* 321.10 (M+2, ~30%).

***In-vitro* Anti-inflammatory activity**

Albumin Denaturation Assay

The synthesized pyrazole derivatives were evaluated for their *in-vitro* anti-inflammatory activity using the heat-induced protein denaturation assay. In this method, bovine serum albumin served as a model protein, and the ability of the compounds to inhibit thermal denaturation was determined spectrophotometrically at 660 nm. Diclofenac sodium was used as the reference standard. All the compounds exhibited dose-dependent inhibition of protein denaturation, showing significant anti-inflammatory potential.

Sl no	Code	Structure	IC50 value (µg/ml)
1	**C1**	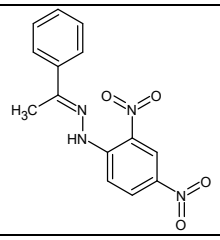	85.42
2	**C2**	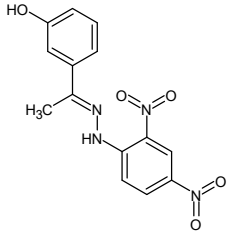	62.83
3	**C6**	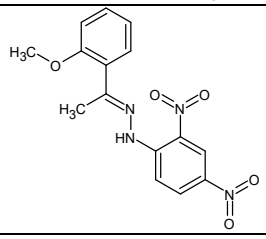	58.16
4	**C7**	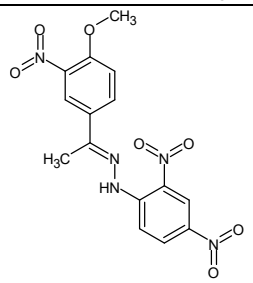	47.65

5	**C9**	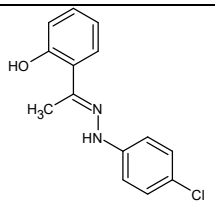	69.93
6	**C10**	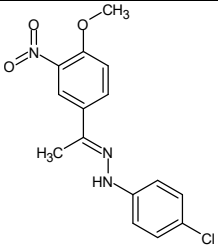	54.22
7	**Standard**	Diclofenac	41.80

Table 4: Result of *in-vitro* anti-inflammatory activity of Hydrazone derivatives by protein denaturation assay

Among the tested compounds, C7 (4-OCH_3, 3-NO_2 substituent) showed the highest activity with an IC_{50} value of 47.65 µg/mL, which was comparable to that of diclofenac (IC_{50} = 41.80 µg/mL). Compounds C6 and C10, having methoxy and nitro groups on the aromatic ring, also demonstrated strong activity with IC_{50} values of 58.16 µg/mL and 54.22 µg/mL, respectively. C2 containing a meta-hydroxyl group showed moderate activity (IC_{50} = 62.83 µg/mL), whereas the chloro-substituted derivative C9 showed moderate inhibition with an IC_{50} of 69.93 µg/mL. The least activity was shown by C1 (IC_{50} = 85.42 µg/mL), which lacks electron-donating substituents. Overall, the presence of electron-donating methoxy and electron-withdrawing nitro groups seemed to enhance anti-inflammatory activity, possibly due to better stabilization of the protein structure or increased interaction with albumin. Thus, compound C7 emerged as the most potent anti-inflammatory agent among the synthesized series.

CONCLUSION

The present investigation successfully demonstrated the design, synthesis and biological evaluation of some series of hydrazone derivatives as potential anti-inflammatory agents. Molecular docking studies against Pokeweed inflammatory Protein (PDB ID: 3O8Y) indicated favorable binding affinities for all designed ligands, with binding energies ranging from -6.3 to -7.2 kcal/mol. These values were largely comparable to the native ligand and highlighted the importance of both hydrogen bonding and hydrophobic interactions in stabilizing the ligand-protein complexes. Among the series, compound C1 exhibited the lowest docking score (-7.2 kcal/mol), forming three hydrogen bonds, suggesting a potentially high affinity toward the inflammatory protein target.

Six compounds (C1, C2, C6, C7, C9 and C10) were synthesized and characterized by IR, NMR and mass spectrometry, confirming the proposed structures. The physicochemical data, such as melting points and percent yields, were consistent with the expected purity profiles.

In-vitro anti-inflammatory activity was assessed by albumin denaturation assay, revealing significant inhibition in a concentration-dependent manner. Compound C7 displayed the most potent activity with an IC_{50} value of 47.65 µg/mL, closely approaching that of standard diclofenac (41.80 µg/mL). Compounds containing both electron-donating methoxy and electron-withdrawing nitro groups showed enhanced activity, indicating that synergistic electronic effects influence protein inhibition capability. Overall, this study establishes hydrazone scaffolds, particularly C7, as promising leads for the development of safer and effective anti-inflammatory agents.

REFERENCES

[1] Zlatanova-Tenisheva H, Vladimirova S. Pharmacological Evaluation of Novel Hydrazide and Hydrazone Derivatives: Anti-Inflammatory and Analgesic Potential in Preclinical Models. Molecules. 2025 Mar 26;30(7):1472-82.

[2] Kamat V, Venuprasad KD, Shadakshari AJ, Bhat RS, D'souza A, Chapi S, Kumar A, Kuthe PV, Sankaranarayanan M, Venugopala KN. Synthesis, anti-inflammatory, antibacterial, and antioxidant

evaluation of novel pyrazole-linked hydrazone derivatives. Journal of Molecular Structure. 2024;1312(1):138634-41.

[3] Ramos KR, Silva JD, de Sousa RS, de Oliveira Borba EF, de Farias Silva MG, Albino SL, Paz ST, da Silva RS, Peixoto CA, Dos Santos VL, Moura RO. N-acyl hydrazone derivatives reduce pro-inflammatory cytokines, iNOS and COX-2 in acute lung inflammation model. Chemico-Biological Interactions. 2025 Jul 29:111677.

[4] Mali SN, Pandey A. Synthesis, computational analysis, antimicrobial, antioxidant, trypan blue exclusion assay, β-hematin assay and anti-inflammatory studies of some hydrazones (Part-I). Current Computer-Aided Drug Design. 2023 Apr 1;19(2):108-22.

[5] Gawali R, Bhosale R, Bavi R, Jadhav S, Peerzade N. Synthesis, Molecular docking studies and biological evaluation of thiazolyl hydrazone derivatives of chromone-3-carbaldehyde as potent anti-oxidant and anti-inflammatory agents. Medicinal Chemistry. 2024 Oct 1;20(8):818-30.

[6] Taxak B, Devi J, Dubey A, Kumar B, Tufail A, Pachwania S, Boora A. Investigation of anti-inflammatory and antimicrobial activities of hydrazone-based diorganotin (IV) complexes: Synthesis, spectroscopic characterization, and computational studies. Applied Organometallic Chemistry. 2024 Feb;38(2):e7323.

[7] Belyaeva ER, Myasoedova YV, Ishmuratova NM, Ishmuratov GY. Synthesis and biological activity of N-acylhydrazones. Russian Journal of Bioorganic Chemistry. 2022 Dec;48(6):1123-50.

[8] Agbo EN, Segodi RS, Gumede NJ, Poopedi KW, Leboho TC, Nxumalo W. Synthesis, in vitro enzyme kinetics and molecular docking studies of the 2-formylphenyl sulfonates and their hydrazone derivatives as potential anti-diabetic and anti-inflammatory agents. Results in Chemistry. 2024 Jan 1;7:101453.

[9] Munir A, Khushal A, Saeed K, Sadiq A, Ullah R, Ali G, Ashraf Z, Mughal EU, Jan MS, Rashid U, Hussain I. Synthesis, in-vitro, in-vivo anti-inflammatory activities and molecular docking studies of acyl and salicylic acid hydrazide derivatives. Bioorganic chemistry. 2020 Nov 1;104:104168.

[10] Bharanidharan M, Manivarman S, Prabakaran G. Catalytic synthesis, in-vitro anti-inflammatory activity, and molecular docking studies of novel hydrazone derivatives bearing N and S-heterocycles. Materials Today: Proceedings. 2022 Jan 1;48:357-64.

[11] Babalola S, Igie N, Odeyemi I. Structure-based discovery of multitarget directed anti-inflammatory p-nitrophenyl hydrazones; molecular docking, drug-likeness, in-silico pharmacokinetics, and toxicity studies.

[12] Raut DG, Bhosale RB, Lawand AS, Hublikar MG, Kadu VD, Patil SB, Choudhari PB. Syntheses, molecular docking and biological evaluation of 2-(2-hydrazinyl) thiazoles as potential antioxidant, anti-inflammatory and significant anticancer agents. Recent Advances in Inflammation & Allergy Drug Discovery. 2022 Sep 1;16(2):96-106.

[13] Wang SM, Zha GF, Rakesh KP, Darshini N, Shubhavathi T, Vivek HK, Mallesha N, Qin HL. Synthesis of benzo [d] thiazole-hydrazone analogues: molecular docking and SAR studies of potential H+/K+ ATPase inhibitors and anti-inflammatory agents. MedChemComm. 2017;8(6):1173-89.

[14] Bozbey İ, Özdemir Z, Uslu H, Özçelik AB, Şenol FS, Orhan İE, Uysal M. A series of new hydrazone derivatives: synthesis, molecular docking and anticholinesterase activity studies. Mini reviews in medicinal chemistry. 2020 Jul 1;20(11):1042-60.

[15] Noshiranzadeh N, Heidari A, Haghi F, Bikas R, Lis T. Chiral lactic hydrazone derivatives as potential bioactive antibacterial agents: Synthesis, spectroscopic, structural and molecular docking studies. Journal of Molecular Structure. 2017 Jan 15;1128:391-9.

[16] Newkome GR, Fishel DL. Synthesis of simple hydrazones of carbonyl compounds by an exchange reaction. The Journal of Organic Chemistry. 1966 Mar;31(3):677-81.

[17] RAIFORD LC, GUNDY GV. α, β-unsaturated ketones obtained from acetophenone, and their reaction with phenylhydrazine. The Journal of Organic Chemistry. 1938;3(3):265-72.

[18] Mali SN, Pandey A. Synthesis, computational analysis, antimicrobial, antioxidant, trypan blue exclusion assay, β-hematin assay and anti-inflammatory studies of some hydrazones (Part-I). Current Computer-Aided Drug Design. 2023 Apr 1;19(2):108-22.

[19] Jadhav SY, Chaugule HN, Alhussain S, Kulkarni AS, Kirdat P, Bavi RS, Bhadange NV, Shekdar VR, Ingle SS, Ghorpade SA, Kadampalle UM. Design, Synthesis and Molecular Docking Study of Piperazine-Linked Imidazo [2, 1-B] Thiazole Derivatives as Potent Anticancer, Antioxidant and Anti-Inflammatory Agents. Antioxidant and Anti-Inflammatory Agents.

[20] Pearlin B. Evaluation of Postbiotics on Production Performance and Endotoxin Challenge in Broiler Chicken as an Alternative to Antibiotic Growth Promoter (AGP) (Doctoral dissertation, Indian Veterinary Research Institute).